Antiferro- to ferromagnetic crossover in diphenoxido bridged Ni$^{II}_2$Mn^{II} complexes derived from N$_2$O$_2$ donor Schiff base ligands

Piya Seth,[a,b] Albert Figuerola,*[c,d] Jesús Jover,[c,e] Eliseo Ruiz,[c,e] and Ashutosh Ghosh*[a]

[a] *Department of Chemistry, University College of Science, University of Calcutta, 92, A.P.C. Road, Kolkata-700 009, India; e-mail:* ghosh_59@yahoo.com

[b] *Sister Nibedita Govt. General Degree College for Girls, Hastings House, 20B, Judges Court Road, Kolkata-700027.*

[c] *Departament de Química Inorgànica, Universitat de Barcelona, Martí i Franquès 1-11, 08028 Barcelona, Spain; e-mail: albert.figuerola@qi.ub.edu*

[d] *Institut de Nanociència i Nanotecnologia (IN2UB), Universitat de Barcelona, Martí i Franquès 1-11, 08028 Barcelona, Spain*

[e] *Institut de Recerca de Química Teòrica i Computacional, Universitat de Barcelona, Diagonal 645, E-08028 Barcelona, Spain*

Three new trinuclear Ni^{II}-Mn^{II} complexes have been synthesized using three different "metalloligands" [NiL^1], [NiL^2] and [NiL^3] derived from the Schiff bases H$_2$L^1= N,N'-bis(salicylidene)-1,3-pentanediamine, H$_2$L^2= N,N'–bis(salicylidene)-1,3-propanediamine and H$_2$L^3= N,N'-bis(salicylidene)-1,3,-diaminopropan-2-ol), respectively. In all three complexes, [(NiL^1)$_2$Mn(OOCPh)$_2$(H$_2$O)$_2$]·CH$_3$OH (**1**), [(NiL^2)$_2$Mn(OOCPh)$_2$(CH$_3$OH)$_2$]·CH$_3$OH (**2**) and [(NiL^3)$_2$Mn(OOCPh)$_2$(H$_2$O)$_2$]·CH$_3$OH (**3**), in addition to the double phenoxido bridge, the two terminal Ni^{II} atoms are linked to the central Mn^{II} by means of a *syn-syn* bridging benzoate, giving rise to a linear structure. Complex **1** with Ni-O-Mn angle of 97.35º exhibits antiferromagnetic interactions (J_{Ni-Mn}= -0.60 cm^{-1}) whereas ferromagnetic exchange is observed in **2** and **3** (J_{Ni-Mn} = +2.00 and +1.10 cm^{-1} respectively) having Ni-O-Mn angle 97.34º (in **2**), 97.27º (in **3**). Theoretical calculations have been performed in order to understand the effect of structural parameters that can tune the magnetic properties of such complexes such as small differences in the Ni-O-Mn angle and/or slight variations in intermolecular contacts within the crystal.

Introduction

Synthesis of homometallic complexes of Ni^{II} with salen type Schiff base ligands with a variety of bridging ligands is well documented over the last few decades due to their interesting magnetic properties,[1] catalytic activity[2] and biological relevance.[3] Octahedral Ni^{II} Schiff base complexes with oxido/phenoxido bridges possess magnetic interactions covering a broad range, from antiferromagnetism to ferromagnetism and their magneto-structural correlations reveal interesting trends.[4] The major factor controlling the exchange coupling (J) is the oxido/phenoxido bridging (Ni–O–Ni) angle. From the experimental observations and theoretical calculations, it has been found that as Ni–O–Ni angle increases from 90º, the ferromagnetic coupling decreases and becomes antiferromagnetic at ca. 93.5º for μ_2-O bridged dinuclear Ni^{II} complexes.[5]

Introduction of heterometal in Ni^{II}-Schiff base complexes using "metalloligand" approach is currently of research interest because it may not only drastically change the topologies but also the catalytic, photoluminescent and magnetic properties.[6] Among these complexes, a handful of Ni^{II}-Mn^{II} complexes have been synthesized and structurally characterized.[7,8] However, magnetic properties of only few of these complexes were studied.[8] We, therefore took an initiative to synthesize some Ni^{II}-Mn^{II} complexes with salen type Schiff bases so that we can establish the dependence of magnetic exchange coupling on structural parameters, especially on the phenoxido bridging (Ni-O-Mn) angle. Recently, we reported some linear trinuclear phenoxido and *syn-syn* carboxylato bridged Ni^{II}-Mn^{II} complexes with salen type Schiff bases where the phenoxido bridging angles range from 96.43−98.51º.[9] It has been found that a linear correlation exists between Ni-O-Mn angle and J_{Ni-Mn} values. From the experimental and theoretical results we proposed that the antiferromagnetic to ferromagnetic crossover angle should be ca. 98º for this type of complexes. To verify our predictions, we would like to synthesize similar type of Ni^{II}-Mn^{II} complexes having identical bridging modes with Ni-O-Mn angle close to 98º that would provide with an opportunity to study the effect of small variation of bridging angle on magnetic coupling.

Herein, we report the synthesis, crystal structure, and magnetic properties of three new phenoxido and *syn-syn* benzoato bridged Ni^{II}-Mn^{II} complexes derived from three closely related Schiff base ligands H_2L^1= N,N'-bis(salicylidene)-1,3-pentanediamine, H_2L^2= N,N'–

bis(salicylidene)-1,3-propanediamine and H_2L^3= N,N'-bis(salicylidene)-1,3,-diaminopropan-2-ol. The complexes are $[(NiL^1)_2Mn(OOCPh)_2(H_2O)_2]\cdot CH_3OH$ (**1**), $[(NiL^2)_2Mn(OOCPh)_2(CH_3OH)_2]\cdot CH_3OH$ (**2**) and $[(NiL^3)_2Mn(OOCPh)_2(H_2O)_2]\cdot CH_3OH$ (**3**). The Ni-O-Mn values for these complexes are 97.35º (in **1**), 97.34º (in **2**), 97.27º (in **3**). Variable temperature magnetic susceptibility measurements exhibit clear antiferromagnetic interactions between Ni^{II} and Mn^{II} ions in **1**, while ferromagnetic exchange is observed in **2** and **3**. Theoretical DFT calculations have been performed in order to analyze the fact that small differences in the Ni-O-Mn angle can tune the magnetic properties of such complexes.

Experimental section

Starting materials

Salicylaldehyde, 1,3-diaminopentane, 1,3-diaminopropane, 1,3-diaminopropan-2-ol, and benzoic acid were purchased from Lancaster and were of AR grade and used without further purification. Manganese benzoate $[Mn(OOCPh)_2\cdot 4H_2O]$ was synthesized by a reported procedure.[10a]

Synthesis of the Schiff-Base Ligands N,N'-bis(salicylidene)-1,3-pentanediamine (H_2L^1), N,N'–bis(salicylidene)-1,3-propanediamine (H_2L^2), and N,N'-bis(salicylidene)-1,3,-diaminopropan-2-ol (H_2L^3)

Three di-Schiff base ligands, H_2L^1, H_2L^2 and H_2L^3 were synthesized in our laboratory by standard methods.[10b] Salicylaldehyde (1.05mL, 10 mM) was mixed with respective diammines *viz.* 1,3-diaminopentane (0.596 mL, 5 mM), 1,3-propanediamine (0.42 mL, 5 mM), 1,3-diaminopropan-2-ol (0.295 g, 5 mM) in methanol (20 mL) and the resulting mixtures were refluxed for *ca.* 1.5 h and allowed to cool to room temperature. The desired yellow crystalline ligands were filtered off from each solution, washed with methanol, and dried in a vacuum desiccator containing anhydrous $CaCl_2$.

Synthesis of the 'metalloligands' [NiL¹], [NiL²] and [NiL³]

Three metalloligands have been prepared by following the same procedure. A mixture of the required di-Schiff base ligand H_2L^1 (1.54 g, 5mM), H_2L^2 (1.432 g, 5 mM) and H_2L^3 (1.49 g, 5mM) in methanol and aqueous ammonia solution (10 mL, 20%) were added to a methanolic

solution (20 mL) of $Ni(ClO_4)_2 \cdot 6H_2O$ (1.825 g, 5 mM) to prepare the desired 'metalloligand' $[NiL^1]$, $[NiL^2]$ and $[NiL^3]$, respectively as previously reported.[11]

Synthesis of complexes $[(NiL^1)_2Mn(OOCPh)_2(H_2O)_2]\cdot CH_3OH$ (1), $[(NiL^2)_2Mn(OOCPh)_2(CH_3OH)_2]\cdot CH_3OH$ (2) and $[(NiL^3)_2Mn(OOCPh)_2(H_2O)_2]\cdot CH_3OH$ (3)

To a 20 mL methanolic solution of respective metalloligands i.e. $[NiL^1]$ (0.734 g, 2mM), $[NiL^2]$ (0.680g, 2mM), $[NiL^3]$ (0.710 g, 2mM), a 1:10 H_2O-MeOH (v/v, 10 mL) mixture of $Mn(OOCPh)_2 \cdot 4H_2O$ (0.370 g, 1 mM) was added drop wise. The resulting mixture was stirred for ca 1 h at room temperature. It was filtered and the filtrate was kept in a beaker inside a desiccator. X-ray quality single-crystals of **1-3** appeared at the wall of the respective beakers on evaporation of the solvent after 2-3 days.

Complex 1: Yield: 0.860 g (76%) $C_{54}H_{62}N_4O_{12}Ni_2Mn$ (1131.40): calcd C, 57.32; H, 5.52; N, 4.95; found C, 57.24; H, 5.49; N, 4.88. IR (KBr pellet, cm^{-1}) 1630 ν(C=N), 1554 ν_{as}(COO), 1471 ν_s(COO).

Complex 2: Yield: 0.746 g (68%) $C_{52}H_{53}N_4O_{12}Ni_2Mn$ (1098.30): calcd C, 56.86; H, 4.86; N, 5.10; found C, 56.71; H, 4.82; N, 4.95. IR (KBr pellet, cm^{-1}) 1630 ν(C=N), 1557 ν_{as}(COO), 1401 ν_s(COO).

Complex 3: Yield: 0.786 g (71%) $C_{50}H_{54}N_4O_{14}Ni_2Mn$ (1107.29): calcd C, 54.23; H, 4.92; N, 5.06; found C, 54.21; H, 4.90; N, 4.92. IR (KBr pellet, cm^{-1}) 1635 ν(C=N), 1564 ν_{as}(COO), 1474 ν_s(COO).

Physical measurements

Elemental analyses (C, H, and N) were performed using a Perkin-Elmer 240C elemental analyzer. IR spectra in KBr (4000–500 cm^{-1}) were recorded using a Perkin-Elmer RXI FTIR spectrophotometer. Temperature-dependent molar susceptibility measurements of polycrystalline samples of **1-3** were carried out at the ''Servei de Magnetoquímica (Universitat de Barcelona)'' in a Quantum Design SQUID MPMSXL susceptometer with an applied field of 3000 and 198 G in the temperature ranges 2–300 and 2–30 K, respectively.

Computational details: To calculate the exchange interactions, a phenomenological Heisenberg-Dirac-van Vleck Hamiltonian was used, excluding the terms relating to magnetic anisotropy, to describe the exchange coupling in a general polynuclear complex:

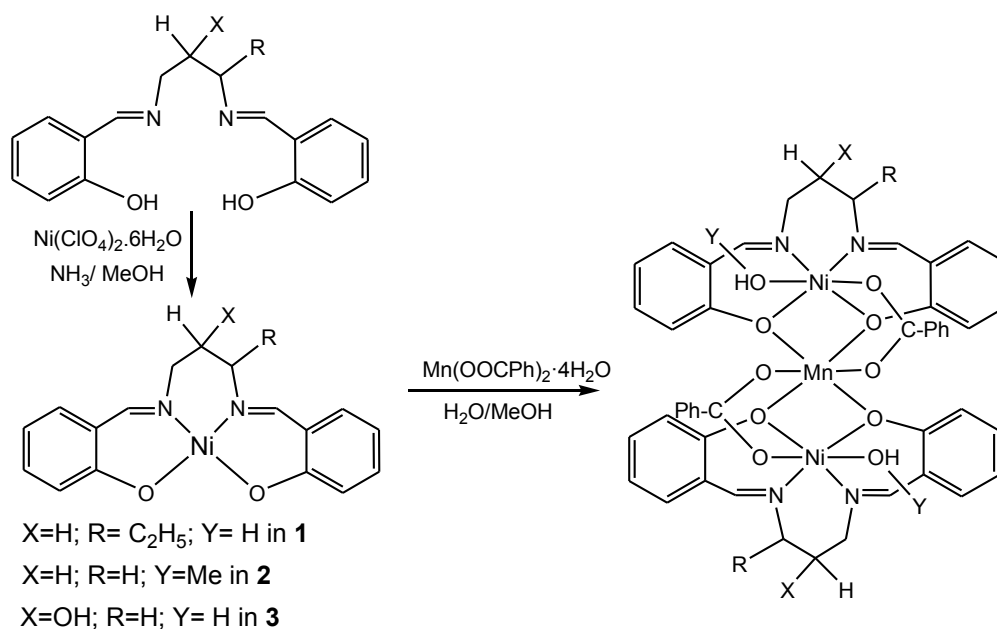$$\hat{H} = -\sum_{a<b} J_{ab}\hat{S}_a\hat{S}_b \qquad (1)$$

where $\hat{S}_a$ and $\hat{S}_b$ are the spin operators of the different paramagnetic cations. The J_{ab} parameters are the pairwise coupling constants between the paramagnetic centres of the molecule. Basically, we need to calculate the energy of $n+1$ spin distributions for a system with n different exchange coupling constants.[12] These energy values allow us to build up a system of n equations in which the J values are the unknowns. In the present study, three calculations were performed in order to obtain the two exchange coupling constants of the MnNi$_2$ complexes. They correspond to the high-spin S = 9/2 state, one S = 1/2 wave function flipping the spin of the central manganese atom, and finally one S = 5/2 with the spin inversion of the two external nickel atoms. Theoretical Calculations were performed with the hybrid B3LYP functional[13] as implemented in Gaussian09 code[14] which employs a procedure that allows us to determine individually the local charges and multiplicities of the atoms, including the ligand field effects.[15]

Crystal data collection and refinement: Suitable single crystals of complexes **1-3** were mounted on a Bruker-AXS SMART APEX II diffractometer equipped with a graphite monochromator and Mo-Kα (λ = 0.71073 Å) radiation. The crystals were positioned at 60 mm from the CCD. 360 Frames were measured with a counting time of 10 s. The structures were solved by the Patterson method using the SHELXS 97. Subsequent difference Fourier synthesis and least-square refinement revealed the positions of the remaining non-hydrogen atoms that were refined with independent anisotropic displacement parameters. Hydrogen atoms were placed in idealized positions and their displacement parameters were fixed to be 1.2 times larger than those of the attached non-hydrogen atom. Absorption corrections were carried out using the SADABS program.[16] All calculations were carried out using the SHELXS 97,[17] SHELXL 97,[18] PLATON 99,[19] ORTEP-32[20] and WinGX system Ver-1.64.[21] Data collection, structure refinement parameters and crystallographic data for the three complexes are given in Table 1.

Results and Discussion

Syntheses, IR and electronic spectra of the complexes

Three new trinuclear heterometallic Ni^{II}-Mn^{II} benzoato bridged complexes derived from three different tetradentate Schiff base ligands have been synthesized. For this purpose, we have first prepared the required Schiff bases in the laboratory following the reported procedure[10b] and then synthesized the respective 'metalloligands' $[NiL^1]$, $[NiL^2]$ and $[NiL^3]$ using these Schiff bases. These 'metalloligands' on reaction with $Mn(OOCPh)_2 \cdot 4H_2O$ (0.370 g, 1 mM) in H_2O-MeOH solvent yielded the desired linear trinuclear diphenoxido and benzoato bridged complexes **1-3** (Scheme 1). Besides elemental analysis, all three complexes were characterized by IR spectroscopy. All three complexes exhibit a strong and sharp band at 1630-1635 cm^{-1}, due to azomethine $\nu(C=N)$. Other peaks due to asymmetric and symmetric stretching of carboxylate are observed at 1554, 1471 cm^{-1} (in **1**) 1557, 1401 cm^{-1} (in **2**) 1564, 1474 cm^{-1} (in **3**) respectively.

X=H; R= C_2H_5; Y= H in **1**
X=H; R=H; Y=Me in **2**
X=OH; R=H; Y= H in **3**

Scheme 1. Formation of complexes **1–3**.

Structure descriptions of the complexes

All three complexes consist of similar structures containing the two terminal Ni^{II} and a central Mn^{II} atoms in a linear disposition. The X-ray crystal structure of **1** reveals that it consists of a

centrosymmetric trinuclear unit $[(NiL^1)_2Mn(OOCPh)_2(H_2O)_2]\cdot CH_3OH$. An ORTEP diagram of **1** is shown in Figure 1 and the selected bond lengths and bond angles are summarized in Table 2. Here, the six-coordinated manganese is in a distorted octahedral environment and is bonded to four oxygen atoms from the two metalloligands $[NiL^1]$, at distances ranging between 2.154(3)-2.168(2) Å that form the basal plane of the Mn^{II}. The *trans* axial positions are occupied by the oxygen atom of the *syn-syn* bridging benzoate ($1\kappa O:2\kappa O'$) at a distance 2.225(2) Å.

The two terminal nickel atoms are bonded to four donor atoms (O(1), O(2), N(1), N(2)) of the ligand L^1, which makes the basal plane with Ni-N distance 2.025(4)-2.048(3) Å and Ni-O distance 2.023(2)-2.031(2) Å. One of the axial positions is occupied by oxygen atom O(4) of the *syn-syn* bridging benzoate at a distance 2.052(3) Å. The other axial position of the nickel atom is bonded to the oxygen atom O(5) of a water molecule at a distance of 2.174(3) Å completing an octahedral geometry around Ni^{II}. The Root-mean-square (r.m.s) deviation shown by four donor atoms in the basal plane from their mean plane is 0.013 Å while the Ni atom is deviated by 0.078(5) Å from the plane towards the carboxylato oxygen O(4). In this complex Ni⋯Mn distance is 3.146(1) Å and the two Ni-O-Mn bridging angle 97.26(9) and 97.47(9)°.
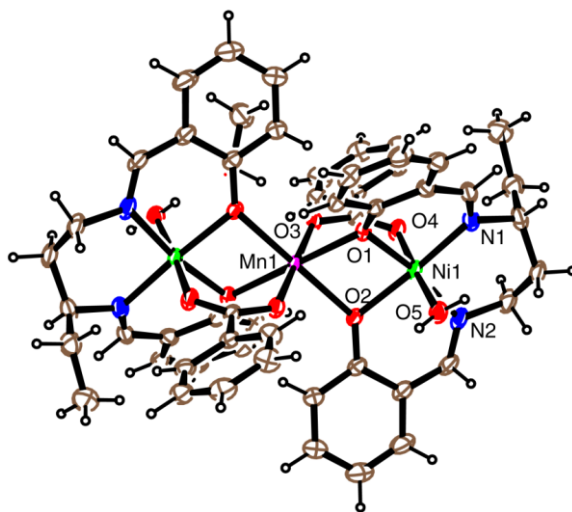

Figure 1. ORTEP-3 view of **1** with ellipsoids at 20% probability.

Complex **2** consists of two similar centrosymmetric trinuclear units **2A** and **2B** having the same composition $[(NiL^2)_2Mn(OOCPh)_2(CH_3OH)_2]\cdot CH_3OH$. An ORTEP diagram of **2A** is shown in Figure 2 and selected bond length and bond angles are summarized in Table 2. Here, both the units contain a six-coordinate central Mn^{II} in a distorted octahedral environment along with two

six-coordinated octahedral Ni^{II} with equivalent geometries at terminal positions. The manganese atom is bonded to four oxygen atoms from the two ligands L^2, at distances ranging between 2.170(2)- 2.176(2) Å in **2A** and 2.162(2)- 2.168(2) Å in **2B**, that form the basal plane of the Mn^{II}. Two trans axial positions are occupied by the oxygen atoms O(3) (in **2A**) and O(8) (in **2B**) of the *syn-syn* bridging benzoate at distances of 2.223(2) and 2.183(2) Å in **2A** and **2B,** respectively.

The nickel atoms are bonded to four donor atoms (O(1), O(2), N(1), N(2) in **2A** and (O(6), O(7), N(3), N(4) in **2B**) of the ligand L^2, making up the equatorial plane with Ni–O distances in the range of 2.020(2)-2.033(2)Å in **2A**, 2.015(2)-2.018(2)Å in **2B** and Ni–N distances of 2.023(2)-2.029(2)Å in **2A,** 2.023(2)-2.024(2)Å in **2B**. One of the axial positions is occupied by oxygen atom (O(4) in **2A**, O(9) in **2B**) of the *syn-syn* bridging benzoate at distances of 2.079(2) and 2.051(2) Å, respectively. The other axial positions of the nickel atoms are bonded to the oxygen atom of the solvent methanol at distances of 2.151(2) Å in **2A** and 2.253(3) Å in **2B**. The mean deviations of four donor atoms in the basal plane from their respective mean plane are 0.0019 Å (in **2A**), 0.00015 Å (in **2B**) while the Ni atom is deviated by 0.029(1) Å to the direction of the axial O(4) in **2A** and 0.081(1) Å towards O(9) in **2B**. Ni···Mn distance is 3.173 Å in **2A** and 3.124 Å in **2B**. Two Ni-O-Mn bridging angles are 97.98(8), 98.15(8)˚ in **2A** and 96.57(8), 96.65(8)˚ in **2B**.
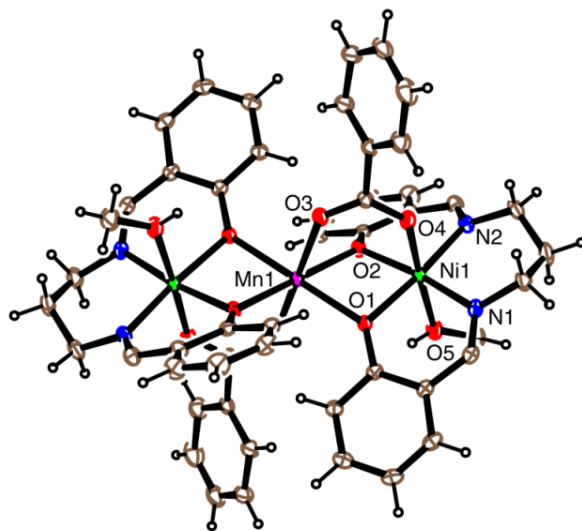

Figure 2. ORTEP-3 view of **2A** with ellipsoids at 20% probability. There are two trimers with equivalent structures, only one is shown.

Complex **3** has the chemical composition $[(NiL^3)_2Mn(OOCPh)_2(H_2O)_2] \cdot CH_3OH$ and its structure is very similar with **1**. An ORTEP diagram of **3** is shown in Figure 3 and the selected bond length and bond angles are summarized in Table 2. Here the central manganese is bonded to four oxygens from the two metalloligands $[NiL^3]$, at distances ranging between 2.167(3)-2.192(3) Å that form the basal plane of the Mn^{II}. The trans axial positions are occupied by the oxygen atom of the *syn-syn* bridging benzoate (1κO:2κO′) at a distance 2.224(3) Å.

The two terminal nickel atoms are bonded to four donor atoms (O(1), O(2), N(1), N(2)) of the ligand L^3, which makes equatorial plane with Ni-N distance 2.022(4) - 2.025(4) Å and Ni-O distance 2.014(3)- 2.030(3) Å. One of the axial positions is occupied by oxygen atom O(4) of the *syn-syn* bridging benzoate at a distance 2.059 (3)Å and the other axial positions is bonded to the oxygen atom O(5) of a water molecule at a distance 2.193(4) Å which is slightly longer than that of **1**. The r.m.s deviation shown by four donor atoms in the basal plane from their respective mean plane is 0.026 Å while the Ni atom is deviated by 0.027(1) Å from the plane towards the carboxylato oxygen O(4). In this complex Ni…Mn distance is 3.159(1) Å and the two Ni-O-Mn bridging angle 97.26(1) and 97.57(1)°.
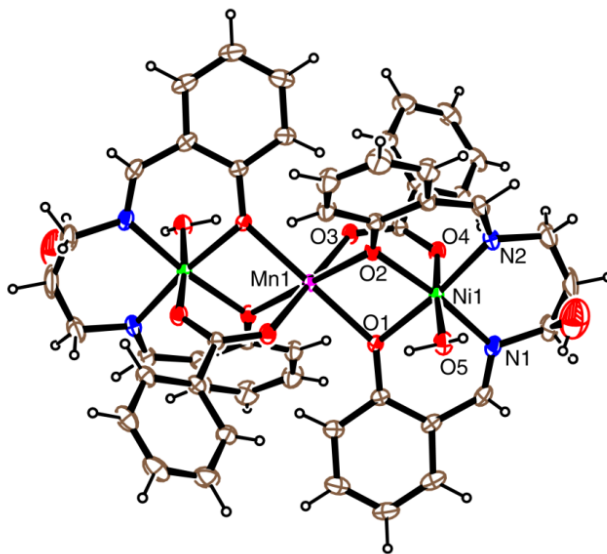

Figure 3. The structure of **3** with ellipsoids at 30% probability.

Magnetic Properties

Magnetic measurements in complex **1** clearly confirm that an antiferromagnetic exchange is operating between Ni^{II} and Mn^{II} ions within this complex. On the contrary, the magnetic interaction is ferromagnetic in nature for complexes **2** and **3**. Temperature-dependent molar susceptibility measurements on polycrystalline samples of **1-3** were carried out in an applied field of 0.3 T in the temperature range 1.9-300 K. The data are shown in the $\chi_M T$ *versus* T plot in Figure 4, where χ_M is the molar magnetic susceptibility and T is the absolute temperature. The room temperature values of $\chi_M T$ for compounds **1-3** are 6.60, 6.64 and 6.66 $cm^3mol^{-1}K$ respectively, slightly higher than the 6.4 $cm^3mol^{-1}K$ value expected for non-interacting Ni^{II}-Mn^{II}-Ni^{II} trinuclear units. The $\chi_M T$ values measured for complex **1** are kept approximately constant down to 100 K, temperature below which they start decreasing gradually reaching a value of 4.10 $cm^3mol^{-1}K$ at 2 K. On the other hand, for complexes **2** and **3**, the $\chi_M T$ values increase with decreasing temperature until they reach a maximum of 7.28 $cm^3mol^{-1}K$ at 15 K for **2** and 8.44 $cm^3mol^{-1}K$ at 5.5 K for **3**. Below these temperatures, the value of $\chi_M T$ drops sharply. In order to quantitatively interpret these data, simulations of the experimental curves were done by using the MAGPACK program as shown in Figure 4.[22] A Hamiltonian of the type $H=-J[S_1S_2+S_1S_3]$, where $S_1 = S_{Mn}$ and $S_2=S_3=S_{Ni}$, was used for the simulations. In the model, the crystallographic equivalence of the two Ni^{II} ions in the trinuclear unit was considered by assigning one single g value for that ion. Additionally, one single set of magnetic parameters was deduced for each of the studied compounds, regardless of the presence of two non-equivalent Ni_2Mn trinuclear molecules in the unit cell in **2**. Simulations were carried out including a zero field splitting (D) value for the two Ni^{II} ions and considering that the exchange coupling between these two terminal ions was zero (J_{Ni-Ni} = 0 cm^{-1}). Moreover, a term accounting for intermolecular interactions (zJ') was also included. The best agreement between experimental and simulated curves was obtained with the following sets of parameters: g_{Ni} = 2.10, g_{Mn} = 2.00, D_{Ni} = 4.0 cm^{-1}, J_{Ni-Mn} = -0.60 cm^{-1} and zJ' = -0.05 cm^{-1} for complex **1**; g_{Ni} = 2.10, g_{Mn} = 2.00, D_{Ni} = 4.0 cm^{-1}, J_{Ni-Mn} = 2.00 cm^{-1} and zJ' = -0.40 cm^{-1} for complex **2**; and g_{Ni} = 2.10, g_{Mn} = 2.00, D_{Ni} = 4.0 cm^{-1}, J_{Ni-Mn} = 1.10 cm^{-1} and zJ' = -0.08 cm^{-1} for complex **3**.
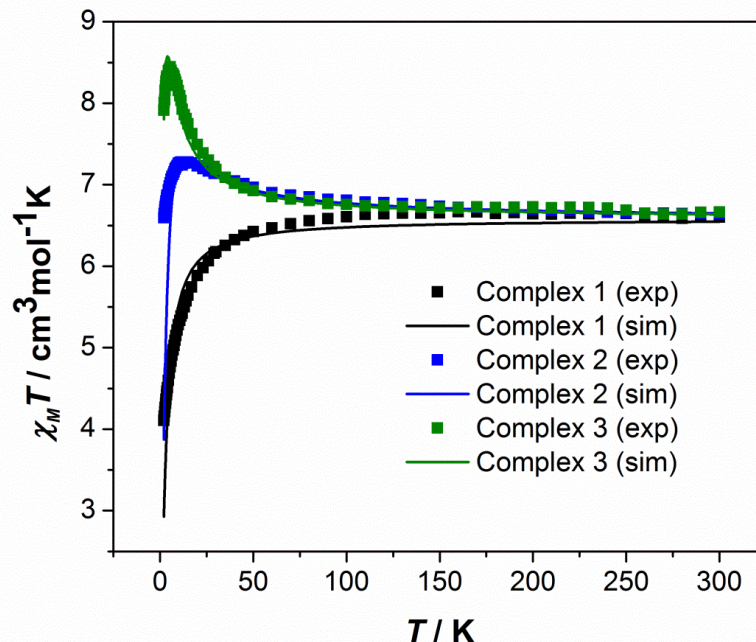
Figure 4. Thermal dependence of the $\chi_M T$ for complexes **1-3**. Symbols represent experimental data while straight lines represent the simulations obtained from the parameters indicated in the main text.

Discussion. We recently reported a magnetostructural study on similar diphenoxido-bridged Ni^{II}_2-Mn^{II} coordination complexes.[9] A linear dependency was found between the J_{Ni-Mn} value and the Ni-O-Mn angle of the monodentate phenoxido bridges, from which a value of the crossover angle from ferro to antiferromagnetic exchange could be assigned. This value corresponds approximately to 98° and apparently indicates that the family of Ni^{II}-Mn^{II} complexes supports ferromagnetic interactions up to angles higher than those observed among other known MM' diphenoxido-bridged complexes, except for the $Mn^{III}Mn^{III}$ family of compounds.[23] Three new diphenoxido-bridged Ni^{II}_2-Mn^{II} complexes (**1-3**) which have been presented in this work, we have described the synthesis and structural characterization possess analogous skeleton to that of previously reported molecules. Thus, it is expected for them to follow a magnetic behavior in agreement with the previously mentioned linear dependency. At first glance, the experimental J_{Ni-Mn} values seem to be consistent with it, showing that these complexes have magnetic exchange couplings of either ferro- or antiferromagnetic nature but always with low magnetic constants in agreement with the values of their Ni-O-Mn angles close to 98°, as shown in Table 3. However, a close look at the data reveals one main discrepancy: the largest ferromagnetic J_{Ni-}

$_{Mn}$ exchange constant corresponds to complex **2**, although this displays an intermediate Ni-O-Mn angle with respect to complexes **1** and **3**. Yet, the very similar Ni-O-Mn angles shown by the three complexes, the difference between the lowest and highest values being 0.08°, do not allow extracting reliable conclusions based only on the previously reported magnetostructural correlation. Additionally, complex **2** contains two non-equivalent molecules in the unit cell with slightly different structural parameters, which will therefore lead to substantially different magnetic exchange constants. Nevertheless, the contribution of each molecule to the bulk average magnetic behavior cannot be ascertained from the measurement performed on crystalline powder. Thus, theoretical calculations have been addressed to better understand the systems.

The experimental (*exp*) and calculated (*calc*) J_{Ni-Mn} magnetic exchange constants for complexes **1-3** are displayed in Table 3, together with their corresponding Ni-O-Mn angle values. The calculations provide average J_{Ni-Mn} values that follow the same trend observed for the experimental ones in all three complexes, confirming that the most ferromagnetic J_{Ni-Mn} constant corresponds to complex **2**, albeit its intermediate Ni-O-Mn angle. Remarkably, the two non-equivalent molecules in complex **2** show significantly different values of the Ni-O-Mn angle, being these 98.07° and 96.61° respectively. Accordingly, calculations performed on single molecules provided an antiferromagnetic J_{Ni-Mn} constant for the former (-0.45 cm^{-1}) and a larger ferromagnetic one (+2.16 cm^{-1}) for the latter, in complete agreement with the expected behavior. Indeed, the calculated J_{Ni-Mn} values follow a linear dependence with the Ni-O-Mn angle as shown in Figure 5 (where two extra data calculated from similar reported structures with extreme Ni-O-Mn angles have been included),[8] suggesting a crossover angle at ca. 98°, in complete agreement with our previous work.[9] All in all, these results evidence the relevance of the Ni-O-Mn angle dictating the strength and nature of the magnetic exchange interaction in such complexes, and further confirm a ferro to antiferromagnetic crossover angle at around 98° for diphenoxido-bridged Ni$^{II}_2$-Mn^{II} coordination compounds. The small deviations from the linear dependency evidence however the presence of secondary structural factors that further tune the magnetic properties of such complexes such as small differences in the Ni-O-Mn angle and/or slight variations in intermolecular contacts within the crystal.
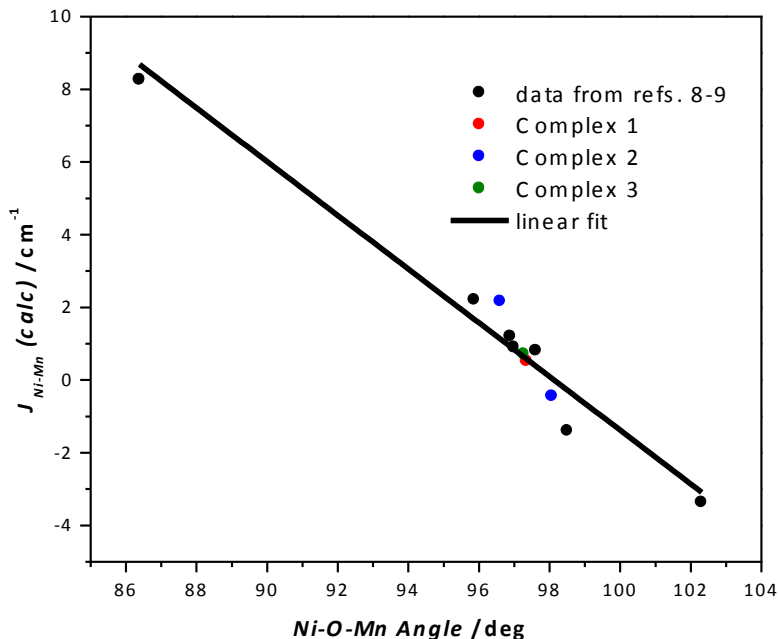
Figure 5. Linear variation of the calculated J_{Ni-Mn} values and the Ni-O-Mn angles of the μ_2-phenoxido bridging ligands for complexes **1**-**3** and for complexes reported in refs. 8, 9. Both parameters have been considered independently for non equivalent molecules contained in complex **2** of this work and complexes **1** and **2** of ref. 9. Additionally, an octahedral coordination environment has been considered in the calculation for Ni[II] ions in complex **2** of ref. 9 for ease of comparison (more details can be found in ref. 9).

Conclusions

Three new diphenoxido and *syn-syn* benzoate bridged Ni[II]-Mn[II] complexes derived from three different salen type Schiff base ligands are synthesized and characterized. All three have similar trinuclear linear structures comprised of a central octahedral Mn[II] and two terminal octahedral Ni[II] atoms having very slight variations in average phenoxido bridging angles (97.27-97.35°). The dependence between magnetic exchange coupling (J_{Ni-Mn}) and phenoxido bridging angle (Ni-O-Mn) has been verified theoretically for this type of complexes, confirming that small differences in this structural parameter are responsible for ferro- or antiferromagnetic interaction between the two metal centers within the complex.

13

Acknowledgements

References

1. a) R. Biswas, Y. Ida, M. L. Baker, S. Biswas, P. Kar, H. Nojiri, T. Ishida and A. Ghosh, *Chem.–Eur. J.,* 2013, **19**, 3943–3953; b) R. Biswas, S. Mukherjee, P. Kar and A. Ghosh, *Inorg. Chem.*, 2012, **51**, 8150–8160.

2. a) K. Yamaguchi, S. Koshino, F. Akagi, M. Suzuki, A. Uehara and S. Suzuki, *J. Am. Chem. Soc.,* 1997, **119**, 5752–5753; b) A. Biswas, L. K. Das, M. G. B. Drew, G. Aromí, P. Gamez and A. Ghosh, *Inorg. Chem.,* 2012, **51**, 7993–8001.

3. a) R. N. Patel, A. Singh, V. P. Sondhiya, Y. Singh, K. K. Shukla, D. K. Patel and R. Pandey, *J. Coord. Chem.*, 2012, **65**, 795–812; b) S. Ciurli, in Metal Ions in Life Sciences, ed. A. Sigel, H. Sigel and R. K. O. Sigel, *John Wiley & Sons, Chichester*, 2007, vol. 2, pp. 241–278.

4. a) K. K. Nanda, R. Das, L. K. Thompson, K. Venkatsubramanian and K. Nag, *Inorg. Chem.,* 1994, 33, 5934–5939; b) R. Biswas, P. Kar, Y. Song and A. Ghosh, *Dalton Trans.* 2011, **40**, 5324–5331; c) R. Biswas, S. Giri, S. K. Saha, and A. Ghosh *Eur. J. Inorg. Chem.* 2012, 2916–2927.

5. A. Burkhardt, E. T. Spielberg, S. Simon, H. Gçrls, A. Buchholz, W. Plass, *Chem. Eur. J.* 2009, **15**, 1261–1271.

6. a) C. Arici, D. Ulku and O. Atakol, *Anal. Sci.* 2002, **18**, 959–960; b) M. Sari, O. Atakol and I. Svoboda, *Anal. Sci.: X-ray Struct. Anal. Online* 2005, **21**, x205–x206; c) O. Atakol, H. Nazir, C. Arici, S. Durmus, I. Svoboda and H. Fuess, *Inorg. Chim. Acta* 2003, **342**, 295–300; d) S. Ghosh, S. Mukherjee, P. Seth, P. S. Mukherjee and A. Ghosh *Dalton Trans.,* 2013, **42**, 13554; e) L. K. Das, A. Biswas, C. J. Gómez-García, M. G. B. Drew and A. Ghosh *Inorg. Chem.* 2014, **53**, 434−445; f) H.-P. Jia, W. Li, Z.-F. Ju and J. Zhang, *Inorg. Chem. Commun.* 2007, **10**, 397–400.

7. a) F. Ercan and O. Atakol, *Acta Crystallogr., Sect. C: Cryst. Struct. Commun.* 1998, **54**, 1268−1270; b) F. Ercan, O. Atakol, C. Arici, I. Svoboda and H. Fuess, *Acta Crystallogr., Sect. C: Cryst. Struct. Commun.* 2002, **58**, m193−m196; c) O. Atakol, H. Nazir, Z. Durmus, I. Svoboda and H. Fuess, *Anal. Sci.* 2002, **18**, 493; d) H. Chen, C. B. Ma, D. Q. Yuan, M.-Q. Hu, H.-M. Wen, Q.-T. Liu and C.-N. Chen, *Inorg. Chem.* 2011, **50**, 10342−10352.

8. a) A. K. Sharma, F. Lloret and R. Mukherjee, *Inorg. Chem.* 2007, **46**, 5128−5130; b) T. Kobayashi, T. Yamaguchi, H. Ohta, Y. Sunatsuki, M. Kojima, N. Re, M. Nonoyama and N. Matsumoto, *Chem. Commun.* 2006, 1950−1952.

9. P. Seth, A. Figuerola, J. Jover, E. Ruiz and A. Ghosh, *Inorg. Chem.* 2014, **53**, 9296-9305.

10. a) W. Ferenc, *Gazz. Chim. Ital.,* 1995, **125**, 23–26; b) J. Reglinski, S. Morris and D. E. Stevenson, *Polyhedron* 2002, **21**, 2167−2174.

11. M. G. B. Drew, R. N. Prasad and R. P. Sharma, *Acta Crystallogr., Sect. C: Cryst. Struct. Commun.* 1985, **41**, 1755−1758.

12. a) E. Ruiz, P. Alemany, S. Alvarez and J. Cano, *J. Am. Chem. Soc.* 1997, **119**, 1297-1303; b) E. Ruiz, *Struct. Bond.* 2004, **113**, 71; c) E. Ruiz, A. Rodríguez-Fortea, J. Cano, S. Alvarez and P. Alemany, *J. Comp. Chem.* 2003, **24**, 982-989; d) E. Ruiz, S. Alvarez, J. Cano and V. Polo, *J. Chem. Phys.* 2005, **123**, 164110; e) E. Ruiz, A. R. Fortea, J. Tercero, T. Cauchy and C. Massobrio, *J. Chem. Phys.* **2005**, *123*, 074102.

13. A. D. Becke, *J. Chem. Phys.* 1993, **98**, 5648–5652.

14. Gaussian 09 (Revision D01): M. J. Frisch, G. W. Trucks, H. B. Schlegel, G. E. Scuseria, M. A. Robb, J. R. Cheeseman, G. Scalmani, V. Barone, B. Mennucci, G. A. Petersson, H. Nakatsuji,

M. Caricato, X. Li, H. P. Hratchian, A. F. zmaylov, I. J. Bloino, G. Zheng, J. L. Sonnenberg, M. Hada, M. Ehara, K. Toyota, R. Fukuda, J. Hasegawa, M. Ishida, T. Nakajima, Y. Honda, O. Kitao, H. Nakai, T. Vreven, J. J. A. Montgomery, J. E. Peralta, F. Ogliaro, M. Bearpark. J. J. Heyd, E. Brothers, K. N. Kudin, V. N. Staroverov, R. Kobayashi, J. Normand, K. Raghavachari, A. Rendell, J. C. Burant, S. S. Iyengar, J. Tomasi, M. Cossi, N. Rega, J. M. Millam, M. Klene, J. E. Knox, J. B. Cross, V. Bakken, C. Adamo, J. Jaramillo, R. Gomperts, R. E. Stratmann, O. Yazyev, A. J. Austin, C. Cammi, J.W. Pomelli, R. Ochterski, R. L. Martin, K. Morokuma, V. G. Zakrzewski, G. A. Voth, P. Salvador, J. J. Dannenberg, S. Dapprich, A. D. Daniels, O. Farkas, J. B. Foresman, J.V. Ortiz, J. Cioslowski, D. J. Fox, Wallingford, CT, 2009. Using a guess function generated with the Jaguar 7.0 code, Jaguar 7.0: Schrödinger, LLC, New York, 2007.

15. G. Vacek, J. K. Perry and J.-M. Langlois, *Chem. Phys. Lett.* 1999, **310**, 189–194. A triple-ζ all-electron Gaussian basis set was used for all the atoms. A. Schaefer, C. Huber and R. Ahlrichs, *J. Chem. Phys.* 1994, **100**, 5829 −5835.

16. SAINT, version 6.02, SADABS, version 2.03, Bruker AXS, Inc., Madison, WI, 2002.

17. G. M. Sheldrick, SHELXS-97, Program for solution of crystal structures, University of Göttingen, Germany, 1997.

18. G. M. Sheldrick, SHELXL-97, Program for refinement of crystal structures, University of Göttingen, Germany, 1997.

19. A. L. Spek, *Acta Crystallogr., Sect. A: Fundam. Crystallogr*., 1990, **46**, C34.

20. L. J. Farrugia, *J. Appl. Crystallogr.,* 1997, **30**, 565.

21. L. J. Farrugia, *J. Appl. Crystallogr.,* 1999, **32**, 837.

22. a) J. J. B. Almenar, J. M. C. Juan, E. Coronado and B. S. Tsukerblat, *J. Comput. Chem.* 2001, **22**, 985-991; b) J. J. B. Almenar, J. M. C. Juan, E. Coronado and B. S. Tsukerblat, *Inorg. Chem.* 1999, **38**, 6081-6088.

23. a) Z. Lu, M. Yuan, F. Pan, S. Gao, D. Zhang, D. Zhu, *Inorg. Chem.* 2006, **45**, 3538−3548; b) G. Bhargavi, M. V. Rajasekharan, J.-P. Costes, J.-P Tuchagues *Polyhedron* 2009, **28**, 1253−1260; c) P. Kar, P. M. Guha, M. G. B. Drew, T. Ishida and A. Ghosh *Eur. J. Inorg. Chem.,*

2011, 2075–2085; d) S. Naiya, S. Biswas, M. G. B. Drew, C. J. Gómez-García, and A. Ghosh *Inorg. Chem.* 2012, **51**, 5332−5341.

Table 1. Crystal data and structure refinement of complexes **1-3**.

	1	2	3
Formula	$C_{54}H_{62}N_4O_{12}Ni_2Mn$	$C_{52}H_{53}N_4O_{12}Ni_2Mn$	$C_{50}H_{54}N_4O_{14}Ni_2Mn$
Formula weight	1131.40	1098.30	1107.29
Space group	P-1	P-1	C2/c
Crystal system	Triclinic	Triclinic	Monoclinic
a/ Å	10.991(5)	10.745(5)	17.497(5)
b/ Å	11.355(5)	11.523(5)	12.968(5)
c/ Å	12.237(5)	21.366(5)	21.787(5)
α/°	74.224(5)	103.842(5)	90.00
β/°	70.492(5)	102.060(5)	97.574(5)
γ/°	69.382(5)	93.906(5)	90.00
V/Å^3	1326.6(1)	2492.4(17)	4900(3)
Z	1	2	4
D_{calc}/g cm^{-3}	1.416	1.464	1.501
Absorption coeff.(μ) mm^{-1}	1.002	1.064	1.086
F(000)	591	1140	2300
R(int)	0.027	0.029	0.034
θ range (deg)	1.8, 29.1	1.0, 26.4	1.9, 26.4
Total reflections	20950	29717	29165,
Unique reflections	6883	9891	4968
$I>2\sigma(I)$	4906	8015	4285
R1, wR2	0.0530, 0.1586	0.0394, 0.1106,	0.0576, 0.1891
Temp (K)	293	293	293

Table 2. Dimensions in the metal coordination spheres in **1-3** (distances,Å, angles,°).

	1	2A	3
Ni(1)−O(1)	2.031(2)	2.020(2)	2.014(3)
Ni(1)−O(2)	2.023(2)	2.033(2)	2.030(3)
Ni(1)−O(4)	2.052(3)	2.079(2)	2.059(3)
Ni(1)−O(5)	2.174(3)	2.151(2)	2.193(4)
Ni(1)−N(1)	2.025(4)	2.023(2)	2.022(4)
Ni(1)−N(2)	2.048(3)	2.029(3)	2.025(4)
Mn(1)−O(1)	2.154(3)	2.176(2)	2.192(3)
Mn(1)−O(2)	2.168(2)	2.170(2)	2.167(3)
Mn(1)−O(3)	2.225(2)	2.223(2)	2.224(3)

O(1)–Ni(1)–O(2)	82.46(9)	82.15(7)	82.56(11)
O(1)–Ni(1)–O(4)	93.50(9)	93.08(8)	92.14(11)
O(1)–Ni(1)–O(5)	88.21(1)	88.67(9)	90.97(12)
O(1)–Ni(1)–N(1)	91.03(1)	91.09(9)	91.16(13)
O(1)–Ni(1)–N(2)	170.66(1)	172.37(11)	172.87(13)
O(2)–Ni(1)–O(4)	91.75(9)	92.70(8)	93.79(11)
O(2)–Ni(1)–O(5)	91.07(1)	89.29(8)	90.14(12)
O(2)–Ni(1)–N(1)	172.69(1)	173.09(9)	173.01(13)
O(2)–Ni(1)–N(2)	89.53(1)	90.39(11)	90.31(13)
O(4)-Ni(1)-O(5)	176.87(1)	177.52(9)	175.28(13)
N(1)–Ni(1)–N(2)	96.66(1)	96.32(12)	95.96(15)
O(4)-Ni(1)-N(2)	91.53(1)	88.90(10)	88.19(14)
O(5)-Ni(1)-N(1)	85.38(13)	89.11(9)	86.88(14)
O(5)-Ni(1)-N(2)	87.14(13)	89.59(10)	89.17(15)
O(1)-Mn(1)-O(2)	76.39(8)	75.57(7)	75.50(10)
O(1)-Mn(1)-O(3)	87.82(9)	88.77(7)	90.38(10)
O(1)-Mn(1)-O(2)[a]	103.61(8)	104.43(7)	104.50(10)
O(1)-Mn(1)-O(3)[a]	92.18(8)	91.23(7)	89.62(10)
O(2)-Mn(1)-O(3)	87.41(8)	83.76(7)	85.07(10)
O(1)[a]-Mn(1)-O(2)	103.61(8)	104.43(7)	104.50(10)
O(2)-Mn(1)-O(3)[a]	92.59(8)	96.24(7)	94.93(10)
O(1)[a]-Mn(1)-O(3)	92.18(9)	91.23(7)	89.62(10)
O(2)[a]-Mn(1)-O(3)	92.59(8)	96.24(7)	94.93(10)
O(1)[a]-Mn(1)-O(2)[a]	76.39(8)	75.57(7)	75.50(10)
O(1)[a]-Mn(1)-O(3)[a]	87.82(9)	88.77(7)	90.38(10)
Ni(1)–O(1)–Mn(1)	97.47(9)	98.15(8)	97.26(11)
Ni(1)–O(2)–Mn(1)	97.26(9)	97.98(8)	97.57(11)

[a] represents symmetry element 2-x,1-y,1-z for **1**, 1-x,-y,1-z for **2A**, 3/2-x,1/2-y,1-z for **3**.

	2B		**2B**
Ni(2)-O(6)	2.015(2)	Ni(2)-N(4)	2.023(2)
Ni(2)-O(7)	2.018(2)	Mn(2)-O(7)	2.162(2)
Ni(2)-O(9)	2.051(2)	Mn(2)-O(8)	2.183(2)
Ni(2)-O(10)	2.253(3)	Mn(2)-O(6)	2.168(2)
Ni(2)-N(3)	2.024(2)		
O(6)-Ni(2)-O(7)	83.39(8)	O(6)[b]-Mn(2)-O(8)	94.36(7)
O(6)-Ni(2)-O(9)	94.55(8)	O(6)[b]-Mn(2)-O(7)	103.45(7)
O(6)-Ni(2)-O(10)	88.56(9)	O(6)[b]-Mn(2)-O(7)[b]	76.55(7)
O(6)-Ni(2)-N(3)	90.28(9)	O(6)[b]-Mn(2)-O(8)[b]	85.64(7)
O(6)-Mn(2)-O(7)	76.55(7)	O(7)[b]-Mn(2)-O(8)[b]	87.81(7)
O(7)-Ni(2)-O(9)	94.76(8)	O(6)-Mn(2)-O(8)	85.64(7)

O(7)-Ni(2)-O(10)	89.56(10)	O(7)-Mn(2)-O(8)	87.81(7)
O(7)-Ni(2)-N(3)	172.34(9)	Ni(2)-O(6)-Mn(2)	96.57(8)
O(7)-Ni(2)-N(4)	89.54(8)	Ni(2)-O(7)-Mn(2)	96.65(8)
O(7)-Mn(2)-O(8)[b]	92.20(7)		

[b] represents symmetry element 1-x,1-y,2-z for **2B**.

Table 3. Selected Structural Parameters of μ_2-Phenoxido-Bridged Ni$_2$Mn Complexes, Ordered by Decreasing Value of their Average Ni-O-Mn Angle.

Compound	$J_{Ni\text{-}Mn}$ (exp) / cm^{-1}	$J_{Ni\text{-}Mn}$ (calc) / cm^{-1}	Ni-O-Mn angle / deg
[Mn^{II}(Ni^{II}L)$_2$(OAc)$_4$(H$_2$O)$_2$][8a]	-0.30	-3.37 (-0.13)	102.31
Complex 1	-0.60	+0.51 (-0.31)	97.35
Complex 2	+2.00	+0.86	97.34
2A	-	-0.45 (-0.31)	98.07
2B	-	+2.16 (-0.30)	96.61
Complex 3	+1.10	+0.71 (-0.30)	97.27
[Mn^{II}(Ni^{II}L)$_2$]·2CH$_3$OH[8b]	+9.30	+8.26 (-0.30)	86.38

In the $J_{Ni\text{-}Mn}$ **(calc)** column, the numbers in brackets correspond to the calculated $J_{Ni\text{-}Ni}$ values, that is the magnetic exchange constants between Ni^{II} ions that belong to the same molecule.